# The IR-RF alpha-efficiency of K-feldspar

Sebastian Kreutzer, Loïc Martin, Stéphan Stephan Dubernet, Norbert Mercier

# Antibacterial, anti-biofilm activity and mechanism of action of Pancreatin doped Zinc oxide nanoparticles against methicillin resistant *Staphylococcus aureus*.

Satarupa Banerjee[1], KumariVishakha[1], Shatabdi Das[1], Debolina Mukherjee, Jyotsna Mondal, Sandhimita Mondal[1], Arnab Ganguli[1*]

[1] Department of Microbiology, Techno India University, West Bengal

EM-4 Sector-V, Saltlake City, Kolkata, West Bengal, India. Pin code – 700091

* To whom correspondence should be addressed:

Arnab Ganguli (ganguli.arnab009@gmail.com)

**Highlights:**

- Pancreatin coated Zinc oxide nanoparticles (ZnNPs-PK) were prepared and characterized
- ZnNPs-PK shows bactericidal, anti-biofilms anti-motility and anti-virulence activity against methicillin resistant *Staphylococcus aureus* (MRSA)
- ZnNPs-PK treatment makes MRSA more sensitive to vancomycin.
- ZnNPs-PK targets cell membrane and induced ROS generation as mode of action against *MRSA*.
- ZnNPs-PK was found to be nontoxic and shows selective antibacterial action.

## Graphical Abstract:

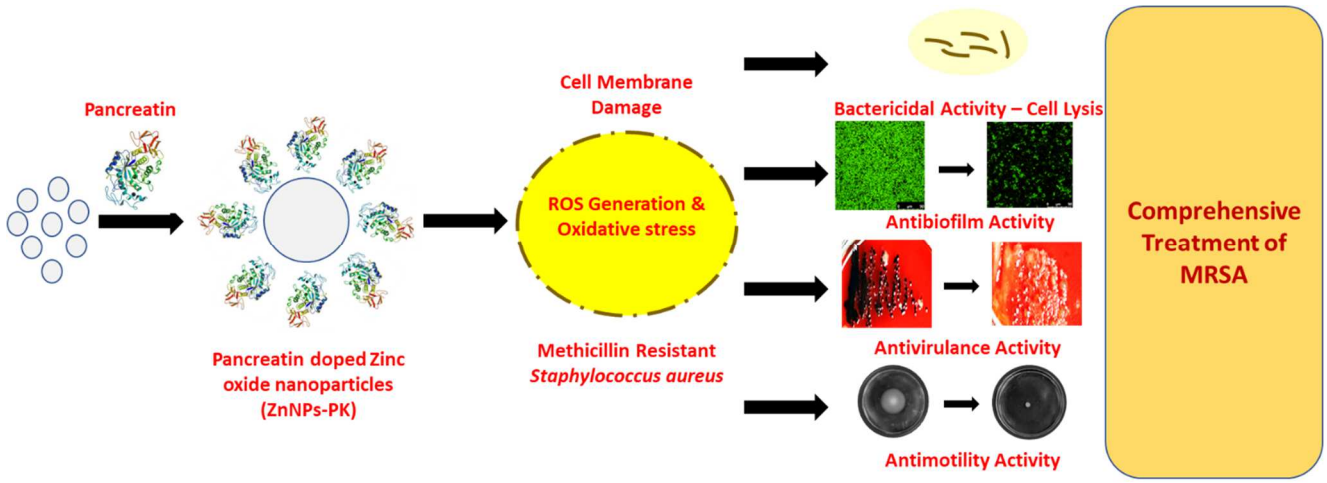

**Abstract**

*Staphylococcus aureus* are known to cause diseases from normal skin wound to life intimidating infections. Among the drug resistant strain, management of methicillin resistant *Staphylococcus aureus* (MRSA) is very difficult by using conventional antibiotic treatment. In present study we show that functionalization of zinc-nanoparticles with pancreatin enzyme have anti-bacterial, anti-biofilms, anti-motility and anti-virulence properties against MRSA. Application of the produced nano-composites as treatment on infected swine dermis predominantly reflects the potential treatment property of it. The vancomycin sensitivity of *MRSA* was significantly increased on application with ZnNPs-PK. Further study revealed ZnNPs-PK targets bacterial cell membrane and induced oxidative damage as its biocidal mode of action. The produced nanoparticles were found completely non-toxic to human's keratinocytes at its bactericidal concentration. Overall, this study emphasizes the potential mechanisms underlying the selective bactericidal properties of Pancreatin doped zinc oxide nanoparticles against MRSA. This novel nanoparticle strategy may provide the ideal solution for comprehensive management of MRSA and its associated diseases with minimising the use of antibiotics.

**Keywords:** Zinc-oxide-Nanoparticles; pancreatin; *MRSA*; Selective-bactericidal; Anti-biofilms;

## 1. Introduction

*Staphylococcus aureus* is a normal micro flora present in humans and results into an opportunistic pathogen with respect to some immuno-suppresive host circumstances[1]. *S. aureus* infections include extremities from normal skin wound to life intimidating infections like pneumonia, and exotoxins syndromes, endocarditis, and septicaemia[1]. Extended and abandoned usage of bacteriostatic or bactericidal antibiotics has also resulted in the emergence of multidrug resistance strains of *S. aureus* (MDR)[2]. Amongst the drug resistant strains, *methicillin resistant Staphylococcus aureus* (*MRSA*) is an exemplar of third generation antibiotic defiant bacteria. The presence of the mecA gene in the staphylococcal cassette chromosome mec is responsible for the methicillin resistant. MRSA could cause broader infection across communities inside and outside of the hospital[3]. MRSA are found to be more resistant to antimicrobial agent than other nosocomial pathogens[4]. Therefore, it becomes tough to be relieved from the infection associated with *MRSA*using conventional antibiotic treatment. This could be a reason why infections associated with *MRSA* have reached pandemic extent worldwide[5].

The existence of various virulence factors such as slime production, exopolysaccharide production, gliding motility, staphyloxanthin pigment production, etc. in *S. aureus* might enhance their probable intimidation particularly that majority of them have enhanced pathogenicity with multi-drug refusal, results it complicated to treat[6]. The most crucial virulence properties of bacteria are the biofilms formation. Biofilms have immense significance for civic wellbeing because of their significant role in spreading of certain contagious diseases[7]. Biofilms associated bacteria are considerably more adaptable to ecological stresses or toxic substances like antibiotics and biocides, than planktonic cells[8]. Therefore, for comprehensive treatment of *MRSA* associated disease, it is important that antibacterial agent should have anti-biofilms and anti virulant properties as well.

Recently, Metal nanoparticles are emerged as a new weapon to combat different bacterial diseases [9]. According to the different metal nanoparticles, Zinc oxide (ZnO) nanoparticles are reported to low cost, bio-safe and much less toxic for human use [10]. Zinc oxide nanoparticles are reported to have broad spectrum antimicrobial activities even act against different drug resistant strains of pathogenic bacteria including *MRSA* [11]. Therefore, zinc oxide nanoparticles may consider as an alternative to conventional antibiotics for the treatment of diseases caused by *MRSA*.

On the other hand, enzymes like Pancreatin also play as great anti-microbial agents[12]. Pancreatin made up of combination of three enzymes – amylase, protease and lipase. It has been reported earlier that, individually these enzymes eliminate biofilms of MRSA[13]–[15]. In addition, this may be a reason for anti-biofilms activity of pancreatin against *MRSA*.

Here in this study, we may hypothesize that ZnO nanoparticles and pancreatin should be a great combination for comprehensive management of *MRSA* associated diseases. For this ZnO nanoparticles were daubed with pancreatin enzymes (ZnNPs-PKs).

Our main objective of this study is to produce a pancreatin daubed zinc oxide nano-composites which produce less toxicity but superior anti-bacterial, anti-biofilm and anti-virulent activity against *MRSA*. To achieve that, in this study we first prepared and characterized ZnNPs-PKs and then investigated how ZnNPs-PKs (I) inhibits growth, (II) affects biofilm formation and other virulence factors of *MRSA*[16].

## 2. Materials and methods:

### 2.1. Micro-organisms:

Clinically isolated culture of methicillin resistant *Staphylococcus aureus* collected from Department of Medical Microbiology, Nil Ratan Sircar Medical College & Hospital, Kolkata, West Bengal, India and maintained in Department of Microbiology, Techno India University, West Bengal was used by growing the bacterial culture on Luria agar, and sub-cultured on Luria Broth prior to each experiment by adjusting turbidity to 0.5 O.D.

### 2.2. Chemicals and compositions:

Analytical grade zinc nitrate $Zn(NO_3)_2 \cdot 6H_2O$;(Sigma-Aldrich-14436) and potassium hydroxide (KOH) (Merck's global life science, Millipore Corporation, USA). Hydrazine hydrate ($N_2H_4$;98.0%) of Sigma-Aldrich (St Louis, MO, USA). Crystal violet solution (99%) of (Merck Merck's global life science, Millipore Corporation, USA) which was used to stain biofilms. 96-wells plates and 12-wells plates (Tarsons Products (P) Ltd.) were used of biofilms inhibition assay.

### 2.3. Synthesis and characterization of nano-composites:

Synthesis of Zinc oxide nanoparticles were prepared by following established protocol [17]. At first, Zinc oxide nanoparticles (ZnNPs) were prepared by precipitation method. Potassium hydroxide solutions (KOH) (0.4M) were slowly added with Zinc nitrate (0.2M) in deionised water at room temperature. The solution was mixed by vigorously stirring until it formed turbid white suspension. The produced white milky suspension was centrifuged at 5000 rpm for 20 minutes and washed thrice with deionised water. Pellet was further washed with ethanol. The resultant product was then calcined in air atmosphere at 500°C for 3 hr. For the preparation of pancreatin daubed zinc oxide nanoparticles (ZnNPs-PK), 2mg/ml pancreatin

enzyme solution was added to the 10mg/ml zinc oxide nanoparticles solution. This was then stirred vigorously under room temperature for 2hrs. After that suspension was centrifuged at 5000 rpm for 20 minutes and washed thrice with deionised water. The prepared nano-composites were the characterized by following way.

To observe the optical property of prepared nanocomposites, samples were analysed for UV–vis spectroscopic studies (UV-visible Spectrophotometer 2206, SYSTRONICS) at room temperature operated at a resolution of 1 nm between 200 to800 nm ranges Dynamic Light Scattering (DLS) analysis was done with a Zeta sizer Nano ZS (Malvern Instruments) according to standard method with some modifications. The amount of enzyme adsorbed on the ZnNPs-PK surface was evaluated by Bradford assay using UV-VIS spectrophotometer.

**2.4. Antibacterial activity of ZnNPs-PK**

**2.4.1 Determination of minimal inhibitory concentration (MIC) and Minimum bactericidal concentration (MBC):**

Determination of minimal inhibitory concentrations (MICs) ofZnNPs and ZnNPs-PK for *MRSA* was determined according to standard protocol lThe bacterial suspension were treated with or without different concentration of ZnNPs-PKs and were incubated at 37°C overnight under shaking condition. After incubation, the MIC values were obtained by checking the turbidity of the bacterial growth. The MIC value corresponded to the concentration that inhibited 99% of bacterial growth[18].

Minimum bactericidal concentration (MBC) was estimated by spreading plating from MIC assay and incubated overnight. The lowest concentration of the nanoparticles which completely killed the tested bacteria was observed and tabulated as MBC value[18].

**2.4.2 Death kinetics:**

To determine the death rate of *MRSA*in presence of ZnNPs-PK, an overnight culture was diluted 100 times in fresh LB and allowed to cultivate at 37◦C under shaking condition upto log phase (~ 5 x $10^7$ cells/ml). ZnNPs-PK was supplemented at MBC and the cells were incubated overnight at 37◦C under shaking condition. At different time interval of 60 mins, cell aliquots were withdrawn, serially diluted and spread on agar plates to evaluate quantity of viable cells[19][20]. According to the slope of the plot (Log $N_t/N_0$ against time associated with incubation), the death rate of ZnNPs-PK treated cells was evaluated[18].

**2.5 Anti-biofilms activity of** ZnNPs-PK

**2.5.1 Initial biofilms inhibition:**

In brief, overnight cultures of *MRSA* were inoculated into wells of a polystyrene 24-well cell culture plate with LB containing various concentrations of ZnNPs-PK and then incubated at 37°C for 24h without agitation. After incubation, LB was removed, and the wells were thoroughly washed with sterile phosphate-buffered saline (PBS) to remove planktonic and non-adherent cells.

For determination of biofilm biomass sessile cells were stained with 0.05% crystal violet, the excess of which was then rinsed off using distilled water. After dissolution with 95% ethanol, the biofilm biomass was determined by reading OD595. The percentage biomass formation was determined using the following equation.

Percentage Biofilm Formation = [{Test Sample OD595 nm/Control sample OD595 nm} ×100].

To investigate cell viability, adherent bacteria in each well were resuspended by vigorous pipetting and vortexing followed by sonication and then were serially diluted $10^6$- through $10^8$-fold and then plated onto LA plates. The agar plates were incubated at 37°C for 24 h before bacterial colonies were counted.

### 2.5.2 Mature biofilms degradation:

Biofilms were cultivated in LB broth in 24-well polystyrene plates at 37°C without shaking. After 24hrsincubation, the broth were removed and the biofilms were rinsed with PBS and then supplemented with fresh LB broth and ZnNPs-PK with different concentrations[20]. After another 24-h cultivation, the formed biofilms were washed with PBS and stained using crystal violet, solubilized with ethanol, and eventually quantified at 595 nm using a microplate reader.

For cell viability, sessile cells were washed with PBS, then resuspended by vigorous pipetting and vortexing and then sonicated for 30 s. The number of CFU/biofilm was quantified by LB agar plating.

### 2.5.3 Microscopic observation of biofilm:

#### 2.5.3.1 Light Microscopy

For light microscopy, the biofilm assay was performed with small glass slides (1×1cm) placed in the wells of the 24-well polystyrene plate. ZnNPs-PK was added at its MIC to the preformed biofilms incubated at 37°C for 24 h. After incubation, planktonic cells were removed, and the biofilm formed on the glass slides was stained using crystal violet dye for 5 min. It was then gently washed with PBS and allowed to dry for 5 min. Then, the slides were viewed under a light microscope at 40x magnification and images were taken using digital camera[21].

#### 2.5.3.2 Confocal Microscopy

The surface topology of *MRSA* biofilm architecture were visualized under Confocal Laser Scanning Microscope (CLSM) by forming biofilm on glass slide placed on 24-well

polystyrene microtiter plate[20]. To determine the effect of ZnNPs-PK to disrupt the mature biofilms, MIC of ZnNPs-PK was added to the mature biofilms and incubated overnight at 37°C, then the glass slides were taken and washed with PBS followed by staining with acridine orange and observed using CLSM (Carl Zeiss LSM700, Jena, Germany)[21].

**2.6. Anti-motility assay:**

**2.6.1 Sliding motility:**

The spreading ability of MRSA on soft LB agar was assessed in the presence and absence of ZnNPs-PK. LB soft agar was prepared with 24 g/1lit of agar and poured into the petri dish plate. Overnight, treated (MIC concentration) and un-treated cultures of MRSA were spotted in the middle of the plate and air dry for 20 mins at room temperature and incubated for 48 hours at 37°C. Sliding motility of selected strains was estimated through measuring the expansion of colony growth from the inoculation point[21].

**2.6.2 Colony spreading assay:**

To determine the anti-colony-spreading activity of ZnNPs-PK 5 ml of LB agar (0.4%) medium with MIC of ZnNPs-PK and without ZnNPs-PK was prepared and then poured over the LB agar plates (2%). After solidification, MRSA were spotted on the centre of the plate and incubated for 24hrs at 37 °C. Further, the diameter of the colony was measured to determine the effect of ZnNPs-PK on spreading[21].

**2.7 Anti-virulence study:**

**2.7.1 Slime production:**

The ability ZnNPs-PK to reduce slime synthesis of *MRSA* was determined by Congo red agar (CRA) analysis. ZnNPs-PK at its MIC was streaked to CRA and was incubated at 37°C for

24 hours. After incubation the changes from black colonies to Bordeaux red colonies was noted. The process was practiced in triplicates[22].

### 2.7.2 Exopolysaccharide production:

To determine EPS production, *MRSA* culture with and without MIC of ZnNPs-PK was grown on LB media in 24 well plate for 24 h at 28 ± 2°C.After incubation, the non-adherent cells were aspirated and removed and 0.5% NaCl was added. These cells suspended in 0.5 % NaCl were transferred to fresh sterile test tubes and added with equal volume of 5% phenol. To that solution, 5 volume of concentrated sulfuric acid containing 0.2% hydrazine sulphate was added and incubated in dark for 1 h and the absorbance was measured at 490nm[23].

### 2.7.3 Staphyloxanthin production assay:

The ability of ZnNPs-PK to reduce the staphyloxanthin pigment secretion was investigated by carotenoid extraction. *MRSA* at its mid log phase were sub-cultured by diluting it to 1:10 (V/V) and ended up to an ultimate volume of 5 ml in LB broth. To the culture, ZnNPs-PK at MIC was added and incubated at 37 °C for 48 hours under shaking conditions. After incubation the cultures were centrifuged at 10,000rpm for 5 mins at 4°C. Culture devoid of ZnNPs-PK was considered as control. The change in color of the culture from golden yellow was measured at an absorbance of 462 nm using UV-VIS spectrophotometer[24].

### 2.7.4 Bacterial Hemolysis activity:

Blood samples of 5mL mixed with acid citrate dextrose to avoid clotting. These samples were first centrifuged, removed the supernatant and then diluted with PBS at 1:10 ratio[25]. Diluted blood samples were inoculated with un-treated and treated bacterial cultures were added to it[20]. These combinations were incubated overnight at 37ºC. Prior to incubation, the tubes were centrifuged at 3,000 rpm for 20 min. Absorbance of supernatants was

calculated at 540 nm and the rate of haemolysis was intended in percentage for the triplicate data[22].

### 2.7.5 Plasma clamping assay:

Overnight cultures of *MRSA* were re-suspended in PBS. Human blood plasma was removed from RBC by centrifugation at 10,000 rpm for 5 minutes. 20µL of plasma was given on the surface of glass slides as small circular drops. In addition, un-treated and treated *MRSA* suspension was added to each of the slides having the plasma samples. Blood plasma with un-treated *MRSA* served as positive control, and plasma with application of distilled water is served as a negative control. The suspensions were blended uniformly macroscopic agglutination of bacterial cells was observed in each trice times[26].

## 2.8 Ex-vivo porcine skin model

Porcine skin majorly includes Swine dermis. Porcine samples were collected from excess trash of local meat shop. The sample was cut in appropriate dimensions (1x1cm) and was surface sterilised with 1% isopropanol for 2hours. The sample skins were place aseptically in sterile stainless-steel clamps having two to three holes for inoculations. Treated and untreated bacterial samples with or without ZnNP-PK were inoculated in the holes of the clamps at MIC and sub-MIC concentrations. Samples treated with sterile media broth were served as negative controls and samples applied with untreated MRSA were served as positive or infective controls. The setups were incubated for 48-72 hours at 37°C. Each setup was experimented in triplicate.

## 2.9. Mechanisms of action:

### 2.9.1 ROS generation:

ROS generation in nanoparticles treated cells were investigated using flow cytometric technique. The $DCFH_2$-DA invade the cell of *MRSA* and combines with ROS to build the highly fluorescent composite 2,7-dichlorofluorescein. After treatment with nanoparticles, *MRSA* were cultured and flashed thoroughly with PBS. The cell pellet was taken and a homogenous suspension up to 1mL was prepared by PBS buffer[27]. Subsequently, the cells were incubated with 1.5 mL of 100 µM $DCFH_2$-DA for 30 min at a temperature of 37ºC. The ROS production was evaluated by flow cytometry (Model: FACSVerse flow cytometer, Becton Dickinson). Data were evaluated by FCSExpress Software.

### 2.9.2 Membrane potential change:

Membrane depolarisation was measured by Rhodamine-123 (Rh123) dye. After treatment with nanoparticles, *MRSA* were cultured and flashed thoroughly with PBS. The cell pellet was taken and a homogenous suspension up to 1mL was prepared by PBS buffer. Rh123 reagent was added and incubated in the dark for 10 minutes and then analysed by flow cytometry (Model: FACSVerse flow cytometer, Becton Dickinson). Data analysed by FCSExpress Software.

### 2.9.3 Membrane Damage:

Propidium Iodide (PI) can enter the bacterial cell membrane only when it has been permeabilized through an agent, and bind with DNA and gives fluorescence. The fluorescence emission can be detected by flow cytometer. After treatment the cells were washed in PBS buffer and incubated with PI (1.3 µg/ml) at 37°C for 20 min in dark. The PI fluorescence was measured in the flow cytometer (Becton Dickinson (BD) FACSVerse). Data analysed by FCSExpress Software.

## 2.10 Combination study of ZnNPs-PK with vancomycin against MRSA

Combination activity of ZnNPs-PK combined with commercial drugs of vancomycin was evaluated against MRSA. For this we first determined the MIC of vancomycin against MRSA. Then MRSA were treated with ¼ and ½ MIC concentration of ZnNPs-PK and vancomycin individually and in combination. The inhibitory activity was determined by checking the turbidity of the bacterial growth. This was measured by spectrophotometrically at a wavelength of 600nm.

### 2.11 Cytotoxicity study on Keratinocytes

HaCaT cells were seeded in 96-well plates at a density of $10^4$cells per well in 0.2 ml of DMEM: Ham's F12 (1:1 v/v) with10% FBS and 1% antibiotics and was cultured at 5% $CO_2$ and37 °C for 24 h [30]. Growth medium inthe wells was replaced after 24 h with medium containing different concentration of ZnNPs-PK and incubated for 24 h.The medium was removed thereafter and replaced with100 µl of medium containing 3-(4, 5-dimethyl-thiazol-2-yl)-2,5-diphenyltetrazolium bromide (MTT) and incubated for4 h. The unreduced MTT was taken out, and 200µl of DMSO was added to each well to dissolve the MTT formazan crystals. The content was mixed properly, and absorbance was measured at 595 nm in a microplate reader.

## 3. Results:

### 3.1. Characterisation of nanoparticles:

The absorption spectra of the ZnNPs (Fig.1A) had a broader band with a maximum at 342nm. After doping with pancreatin we also spectrophotometrically characterized the nanoparticles. The absorption spectrum of ZnNPs-PK showed an increased absorption at 280nm indicating the binding of enzyme to the ZnNPs nanoparticles.

Average particle size, distribution and polydispersity index (PDI) of synthesized Zn-NPs and ZnNPs-PK in solutions were evaluated by DLS technique. The DLS pattern revealed that ZnNPs had a Z average diameter of 5nm. Which was significantly increased to 45nm (Fig.1B). Hence it may hypothesize that binding of pancreatin to ZnNPs increased the particles size of the nanoparticles. The PDI value of the synthesized ZnNPs was 0.641 indicating nearly monodisperse distribution. Little change in the PDI value was observed after the binding with pancreatin, indicating that the size distribution was not affected by the ZnNPs-PK interaction.

The percent of protein adsorbed on the functionalized nanoparticles surface was 0.47 ± 0.4% (W/W) as determined by Bradford assay. That indicates binding of few micrograms of proteins per milligram of nanoparticles.

**3.2 Antibacterial activity of ZnNPs-PK:**

**3.2.1 Determination of minimum inhibitory concentration of ZnNPs and ZnNPs-PK against MRSA**

At first, we determined comparative antibacterial activity of ZnNPs and ZnNPs-PK against the *MRSA* (Fig.2A). For this, we did broth dilution method to determine the minimum inhibitory concentration of ZnNPs and ZnNPs-PK against the *MRSA*. Different concentrations of the nano-composites were used to treat *MRSA* for the estimation of the MIC value. After incubation, spectrophotometric analysis revealed that the MIC90 for ZnNPs and ZnNPs-PK was 75 and 156 µg/mL respectively. This indicates ZnNPs-PK nanoparticles exhibit greater antimicrobial potential than ZnNPs. Thus ZnNPs-PK nano-composites were used to study further antibacterial, anti-biofilms and anti virulence activities against *MRSA*.

To understand the mode of antimicrobial activity, MBC concentration of ZnNPs-PK against *MRSA* was determined. The MBC concentration was found to be 120µg/mL. After that, as previous reports suggests[31], we determined the tolerance value to understand the nature of antimicrobial activity of the nano-composites. The tolerance value was 1.6 indicated bactericidal activities of the ZnNPs- PK against *MRSA*.

### 3.2.2 Death kinetics:

As we found prepared nanoparticles are bactericidal in nature, hence definitely these nanocomposites have an effect on the growth of bacteria and that can be evaluated by investigating the death kinetics of MRSA in presence and absence of ZnNPs-PK. For this we treated *MRSA* with MBC concentration of nanoparticles and subsequently the viable cell counts were measured at different times of exposure up to 6 hours, because significant amount cell killing occur within this period. The rate of death percentage of *MRSA* after the treatment was calculated from slopes of straight-line curve (Fig.2B) to be $0.87h^{-1}$. In the untreated *MRSA* the growth rate was $0.72h^{-1}$. This result strengthened the bactericidal nature of our nano-composites.

## 3.3. Anti-biofilms activity of ZnNPs-PK against *MRSA*

### 3.3.1 Initial biofilms inhibition:

At the initial stage of disease progression, planktonic cells are always trying to attach to the substratum or the surface for colonization. That leads to the formation of biofilm. Therefore, inhibition of this initial attachment may be a key factor for finding promising antibiofilm agents. The effects of ZnNPs-PK on inhibition of initial biofilms formation by MRSA was determined by enumerate viable sessile cells and crystal violet assay. ½ MIC and MIC concentration of ZnNPs-PK treatment reduced the viable sessile cells by 4 and 7log (CFU/well) respectively as compared with control (Fig.3A). Similarly, the biofilms biomass

was also decreased to 50 and 30 % after treatment with MIC and ½ MIC concentration of ZnNPs-PK. (Fig.3A). We also investigated effect of only ZnNPs on initial biofilms formation of *MRSA*. We found at 75µg/ml of ZnNPs treatment could not showed any significant antagonistic effect on survivability of sessile cells of *MRSA*.

### 3.3.2 Preformed biofilms degradation:

As we found an encouraging result about initial biofilm formation inhibition by ZnNPs-PK, we extended our study to understand the disruptive potential of our prepared nanoparticles on preformed biofilms. Prior treatment, we first incubated *MRSA* for 48h to allow the biofilms formation. The ½MIC and MIC concentrations of ZnNPs-PK treatment resulted in a remarkable reduction of the preformed biofilms in *MRSA* (Fig.3A). Similarly, the sessile cells of preformed biofilms were eradicated by ZnNPs-PK in a concentration-dependent manner (Fig.3B).

### 3.3.3 Microscopic observation of biofilms inhibition by ZnNPs-PK:

Both the light and confocal microscopic study confirmed disruption of *MRSA* biofilms by ZnNPs-PK. For light microscopic study, application of crystal violet on the mature biofilms by *MRSA*, untreated and treated with ZnNPs-PK at its MIC concentrations. Biofilms disruption was clearly observed as the untreated samples retained more stains than the treated samples (Fig.3B). The consequence of ZnNPs-PK to disturb the mature biofilms of *MRSA* was also examined with CLSM by using acridine orange staining. It is apparent that there is a decrease of green fluorescence in treated samples when compared to that of control indicating disruption of biofilms. All these data suggest ZnNPs-PK effectively eradicate the bioflim formation of *MRSA*.

### 3.4 Anti-motility activity of ZnNPs-PK against *MRSA*

### 3.4.1 Sliding assay:

Gram-positive MRSA is anon flagellated bacteria, hence they can spread by means of sliding motility and that aided to increased biofilm formation on the surface[32]. Thus, to understand the effect of ZnNPs-PK on sliding motility of MRSA was determined by inoculating a culture of MRSA in presence and absence ofZnNPs-PK on the centre of semisolid growth media and incubated for 48 hrs at37°C. In control, we found the sliding motility was well established, wherein the plates treated with nanoparticles significantly reduced the sliding motility of MRSA (Fig.4A).

### 3.4.2 Colony spreading assay:

In colony spreading assay, we found untreated control MRSA appeared as rapid and expanded colony spreading on the agar surface, whereas ZnNPS-PK treated MRSA showed a notable reduction in spreading as compared to control (Fig.4A).

## 3.5Anti-virulence activity of ZnNPs-PK against *MRSA*

### 3.5.1 Exopolysaccharide and Slime production:

The Slime and exopolysaccharide production by bacteria were considered as key virulent factors for attachment, colonization and biofilm formation within host[33]. Therefore, reduction of both slime and exopolysaccharide production is an important criterion for an anti-biofilm agent. In this study, we evaluated the capability of ZnNPs-PK to reduce the slime and exopolysaccharide production of *MRSA* was analysed by Congo red agar (CRA) test and EPS quantification analysis respectively. In CRA test ZnNPs-PK at its MIC concentration reduced the slime production which was determined by color alteration from black to bordeaux red (Fig.5A). On the other hand, EPS production was spectrophotometrically

quantified in treated and untreated samples. We found EPS production was significantly reduces in MIC treated MRSA as compared to the control (Fig.6A).

### 3.5.2 Staphyloxanthin production assay:

Staphyloxanthin protects *MRSA* from oxidative stress as well as from the host immune system[34]. Therefore, reduction of staphyloxanthin should be an advantageous for an antimicrobial agent. We found in our study, staphyloxanthin production of *MRSA* was significantly reduced at MIC treatment of ZnNPs-PK as in Fig.6A. Therefore, it can be hypothesized that ZnNPs-PK makes susceptible *MRSA* towards oxidative stress.

### 3.5.3 Bacterial Hemolysis activity:

*S. aureus* produces a series of haemolysins which lyses erythrocytes and various leukocytes such as neutrophils, monocytes, granulocytes and macrophages[35]. The effectiveness of ZnNPs-PK to reduce the haemolytic virulence property of *MRSA* strains, erythrocytes was exposed to MRSA with or without treated with ZnNPs-PK. We observed that ZnNPs-PK treated *MRSA* showed anti-hemolytic activity. Up to 80% inhibition in haemolytic activity was detected upon treatment with ZnNPs-PK (Fig.6A).

### 3.5.4 Plasma clamping assay:

Clumping factors are key virulence of *MRSA* for their pathogenicity and survival against host immune system®. In this study, to understand the ability of ZnNPs-PK to inhibit clumping factors of *MRSA*, we evaluated bacterial cell clumping activity using the slide coagulation test with blood plasma.In the absence of nanoparticles, *MRSA*was found to readily agglutinate in blood plasma, whereas in ZnNPs-PK treated *MRSA*, less clumping activity was observed (Fig.5B).

### 3.6 Ex-vivo porcine skin model to understand the anti-infective nature of ZnNPs-PK against *MRSA*

Porcine skin surface was inoculated with MRSA with or without treatment at MIC of ZnNPs-PK. The skin surface was the cultured 24 h for biofilms formation and physical appearance of infections (Fig.8A). The established bioburden was characterized by plating to determine CFU/ml. After 24h, we noted $9.45x10^4$CFU/cm2in untreated skin surface. However, in MIC of ZnNPs-PK treatment significantly reduced the bioburden of *MRSA* to $3x10^4$CFU/$cm^2$.

### 3.7. Mechanisms of action of ZnNPs-PK against *MRSA*

#### 3.7.1 ZnNPs-PK induced the oxidative stress in *MRSA*

Oxidative stress levels in *MRSA* after treatment with ZnNPs-PK was determined by using the 2',7'-dichlorofluorescin diacetate (DCFDA) assay. We noted that by flow cytometric assay mean fluorescence intensity of green fluorescence in *MRSA* treated with MIC of ZNNPs-PK was significantly increased as compared with the untreated cells. This indicates ZNNPs-PK induced oxidative stress by means of ROS generation in *MRSA* and this may be a possible mechanism responsible for the antibacterial effects of nanoparticles (Fig.6B).

#### 3.7.2 Membrane potential change:

Change in membrane potential after treatment with antimicrobial was considered as another antimicrobial mechanism. Membrane potential has a key role in bacterial physiology[36]. Therefore change in membrane potential is an early onset of injury in bacteria. In our study it was evaluated by flow cytometric assay using rhodamine 123. After exposure to ZnNPs-PK at MIC a considerable decrease of MFI values was observed respectively as compared with control (Fig.7A).

#### 3.7.3Membrane Damage:

Next to understand the membrane damage; we used propidium iodide-based flow cytometric method. In untreated *MRSA*, only a small proportion of cells 5% were stained with PI indicating lesser membrane damage. However, after treatment with MIC of ZnNPs-PK, the bacterial cells with damaged membrane stained by PI were increased to 77% (Fig.7B). Therefore, it can be hypothesized that ZnNPs-PK targets bacterial cell membrane for its antimicrobial activity.

### 3.8 Combination study of ZnNPs-PK with vancomycin against MRSA

In our study we found the MIC value of vancomycin against MRSA was 1µg/ml. It has been reported that vancomycin MIC against MRSA in the range of 0.5 to 2 µg/ml would have significant clinical implications®. Therefore, we performed a combination study to understand the effect of ZnNPs-PK on the vancomycin sensitivity to MRSA. We found ¼ MIC concentrations of both antibacterial in combination completely inhibit the growth of MRSA as compared with individual treatment (Fig.8B). Therefore, this signifies that ZnNPs-PK may intensify the sensitivity of vancomycin to MRSA.

### 3.9 Cytotoxicity of ZnNPs-PK on HaCaT (Keratinocytes) cell line

Cytotoxicity of ZnNPs-PK on HaCaT (Keratinocytes) cell line was determined by MTT assay. The IC90 (concentration at which 90% decrease in cell viability was observed) value was found to be 400 µg/ml. The cytotoxic concentration of nanoparticles was found to be 5-fold higher than that of MIC for bacteria (Fig.7C). Selectivity of ZnNPs-PK was calculated by taking the ratio of $IC90_{HaCaT}/MIC_{MRSA}$ and it was found to be 5.33 [37].

### Discussions:

Organisms like MRSA are primarily known for its skin infections. It is a foremost reason of bacteraemia and infective endocarditic problems additionally osteo-articular, skin and

flexible tissue damage[38]. As MRSA is considered as a well-known MDR strain, it is tremendously difficult to be treated to normal ranges of antibiotics. Moreover, next generations of antibiotics also impart toxic side effects on human body[39]. The treatment is further complicated as MRSA are known as strong biofilms producer[40]. The biofilms formations not only increase the resistant against the antibiotic but also prevent antagonistic activities of immune cells of the host[41]. Under these circumstances, it has become very important to produce an alternative way which has efficient antimicrobial as well as antibiofilm effect on the respective strain though having low toxicity. In this study, initially we have been able to produce zinc oxide nanoparticles (ZnNPs). ZnNPs are considered as less toxic, biosafe among the other metal nanoparticles[10]. Further, these nanoparticles have been doped with antibacterial enzyme pancreatin. The initial process of this study includes the characterization of the formed nanoparticles which involves analytical tests like DLS, UV-visible spectroscopy. Both DLS and UV spectra analysis assure the presence of doped pancreatin on the surface of zinc-oxide nanoparticles. The lower MIC value of ZnNPs-PK than ZnNPs suggest pancreatin doping increased the antimicrobial potential of nanoparticles. Tolerance value indicated biocidal activity of ZnNPs-PK, which is further confirmed by death kinetics assay. Inhibition of biofilm formation of pathogenic organisms is also an important criterion for a comprehensive antimicrobial agent [42]. ZnNPs-PK was found to impaired initial and mature biofilms formation of MRSA. It can be hypothesized that, amylase lipase and protease activity of pancreatin degrade the carbohydrate and protein rich biofilms produced by MRSA. After degradation of the biofilms it become easier for the ZnNPs to invade and shows antagonistic activity on the sessile bacterial cell. Motility is an important criterion of bacteria for its initial attachment with substratum and following biofilm formation to disease progression[32]. Therefore, antimotility activity of antibacterial agent should provide an additional advantage for disease management. In our study, ZnNPs-PK

491 inhibit both sliding motility and colony spreading activity of staphylococcus and may
492 consequently inhibit the biofilm formation as reported previously. Like motility, EPS
493 production also plays an important role for bacterial adhesion, adaptation and biofilm
494 formation [33]. EPS production significantly reduced in ZnNPs-PK treated MRSA, which
495 might be the reason for the reduction of biofilm of MRSA.MRSA produce variety of
496 virulence factors for the disease progression [43]. Therefore, inhibition of one or two
497 virulence factors is not enough for a comprehensive treatment. ZnNPs-PK was also found to
498 diminish staphyloxanthin secretion and eventually increase susceptibility of MRSA to
499 oxidative stress and host immune system. Not only that, other two virulence factors those are
500 important for survival within host, such as the haemolytic and plasma clumping activity were
501 significantly reduced in ZnNPs-PK treated MRSA give an idea of anti-infective nature of the
502 nanoparticles. This anti-infective nature of nanoparticles was further assessed by porcine skin
503 model. Where we found bioburden was significantly reduced in ZnNPs-PK treated MRSA
504 infected skin model as compared with control. All these data suggest ZnNPs-PK is an
505 effective antibacterial, anti-biofilms, anti-virulence and anti-infective agent against MRSA.
506 Furthermore, it is important to understand the mechanism associated with antibacterial
507 activities of ZnNPs-PK on MRSA. It has been previously reported that ZnNPs induced ROS
508 generation and targets bacterial membrane [44]. In our study we also found ZnNPs-PK
509 treatment induced significant reduction of membrane potential indicating it may target
510 bacterial cell membrane. Bacterial cell membrane plays a vital role for the survival and
511 growth of the bacteria [45]. Reduction of membrane potential also increased the ROS
512 generation in treated cells and that is similar to previous reports [46]. ROS may oxidize
513 different cellular constituent including proteins, nucleic acid and lipid of the cell membrane.
514 Moreover, lipid oxidation may increase permeability of membrane as we found significant
515 uptake of PI in treated cells than untreated cells. Ultimately damage to membrane may leads

to release of cellular constituents and death of the bacterial cells. This clinical MRSA was found to be intermediate resistance to vancomycin. We found combination treatment of ¼ MIC of both vancomycin and ZnNPs-PK completely inhibited the growth of bacteria. This may indicate synergistic activity of ZnNPs-PK and vancomycin in combination against MRSA. Finally, it is important to understand biosafe nature of the prepared nanoparticles. the IC90 concentration of nanoparticles were five times higher than the MIC of MRSA. The ratio of $IC90_{HaCaT}$and $MIC_{MRSA}$ showed that ZnNPs-PK is selectively cytotoxic towards MRSA as the concentration required to inhibit bacterial growth is much lesser, i.e., 5-fold less than $IC90_{HaCaT}$.

**Conclusions:**

This study concluded that ZnNPs-PK possesses bactericidal, anti-biofilms, anti-motility and anti-virulence properties against MRSA. ZnNPs-PK targets cell membrane and increased oxidative stress as its mode of action against MRSA. It increased the vancomycin sensitivity of our clinical MRSA strain. ZnNPs-PK was found to nontoxic with selective bactericidal properties. In a nutshell, ZnNPs-PK can be used for comprehensive treatment of diseases associated with MRSA.

**3. Acknowledgements:**

The authors are thankful to Chancellor, Techno India University, West Bengal for providing the necessary infrastructural and laboratory facilities. The authors are also thankful to Dr. Ritesh Tiwari for supporting flow cytometry facilities at Centre for research in Nanoscience and Nanotechnology (CRNN), University of Calcutta.

**Conflict of interest:**

The authors declare that there is no conflict of interests regarding the publication of this paper.

## 4. References:


[1] J. P. O'Gara, 'Into the storm: Chasing the opportunistic pathogen Staphylococcus aureus from skin colonisation to life-threatening infections', *Environ. Microbiol.*, vol. 19, no. 10, pp. 3823–3833, 2017.

[2] M. E. A. de Kraker, P. G. Davey, H. Grundmann, and BURDEN study group, 'Mortality and hospital stay associated with resistant Staphylococcus aureus and Escherichia coli bacteremia: estimating the burden of antibiotic resistance in Europe', *PLoS Med.*, vol. 8, no. 10, p. e1001104, Oct. 2011.

[3] H. C. Neu, 'The crisis in antibiotic resistance', *Science*, vol. 257, no. 5073, pp. 1064–1073, Aug. 1992.

[4] M. Z. David and R. S. Daum, 'Update on Epidemiology and Treatment of MRSA Infections in Children', *Curr Pediatr Rep*, vol. 1, no. 3, pp. 170–181, Sep. 2013.

[5] S. Monecke *et al.*, 'A field guide to pandemic, epidemic and sporadic clones of methicillin-resistant Staphylococcus aureus', *PLoS ONE*, vol. 6, no. 4, p. e17936, Apr. 2011.

[6] R. J. Gordon and F. D. Lowy, 'Pathogenesis of Methicillin-Resistant *Staphylococcus aureus* Infection', *CLIN INFECT DIS*, vol. 46, no. S5, pp. S350–S359, Jun. 2008.

[7] M. K. Luther *et al.*, 'Clinical and Genetic Risk Factors for Biofilm-Forming *Staphylococcus aureus*', *Antimicrob Agents Chemother*, vol. 62, no. 5, pp. e02252-17, /aac/62/5/e02252-17.atom, Mar. 2018.

[8] A. Kumar, A. Alam, M. Rani, N. Z. Ehtesham, and S. E. Hasnain, 'Biofilms: Survival and defense strategy for pathogens', *Int. J. Med. Microbiol.*, vol. 307, no. 8, pp. 481–489, Dec. 2017.

[9] U. Kadiyala, N. A. Kotov, and J. S. VanEpps, 'Antibacterial Metal Oxide Nanoparticles: Challenges in Interpreting the Literature', *Curr. Pharm. Des.*, vol. 24, no. 8, pp. 896–903, 2018.

[10] P. K. Mishra, H. Mishra, A. Ekielski, S. Talegaonkar, and B. Vaidya, 'Zinc oxide nanoparticles: a promising nanomaterial for biomedical applications', *Drug Discov. Today*, vol. 22, no. 12, pp. 1825–1834, 2017.

[11] A. Sirelkhatim *et al.*, 'Review on Zinc Oxide Nanoparticles: Antibacterial Activity and Toxicity Mechanism', *Nanomicro Lett*, vol. 7, no. 3, pp. 219–242, 2015.

[12] R. Scheer and A. A. Fawzy, 'Antimicrobial treatment of pancreatin', *Pharm Acta Helv*, vol. 61, no. 9, pp. 253–256, 1986.

[13] B. Craigen, A. Dashiff, and D. E. Kadouri, 'The Use of Commercially Available Alpha-Amylase Compounds to Inhibit and Remove Staphylococcus aureus Biofilms', *Open Microbiol J*, vol. 5, pp. 21–31, 2011.

[14] S. Shukla and Ts. Rao, '*Staphylococcus aureus* biofilm removal by targeting biofilm-associated extracellular proteins', *Indian J Med Res*, vol. 146, no. 7, p. 1, 2017.

[15] V. Prabhawathi, T. Boobalan, P. M. Sivakumar, and M. Doble, 'Antibiofilm Properties of Interfacially Active Lipase Immobilized Porous Polycaprolactam Prepared by LB Technique', *PLoS ONE*, vol. 9, no. 5, p. e96152, May 2014.

[16] J. Schulz, A. Boklund, N. Toft, and T. Halasa, 'Risk-based eradication as a control measure to limit the spread of LA-MRSA among Danish pig herds - a simulation study', *Sci Rep*, vol. 9, no. 1, p. 13192, Sep. 2019.

[17] R. Herrera-Rivera, M. de la L. Olvera, and A. Maldonado, 'Synthesis of ZnO Nanopowders by the Homogeneous Precipitation Method: Use of Taguchi's Method for Analyzing the Effect of Different Variables', *Journal of Nanomaterials*, vol. 2017, pp. 1–9, 2017.

[18] R. Mukherjee, M. Patra, D. Dutta, M. Banik, and T. Basu, 'Tetracycline-loaded calcium phosphate nanoparticle (Tet-CPNP): Rejuvenation of an obsolete antibiotic to further action', *Biochim. Biophys. Acta*, vol. 1860, no. 9, pp. 1929–1941, 2016.
[19] L. de Sousa Eduardo, T. C. Farias, S. B. Ferreira, P. B. Ferreira, Z. N. Lima, and S. B. Ferreira, 'Antibacterial Activity and Time-kill Kinetics of Positive Enantiomer of α-pinene Against Strains of Staphylococcus aureus and Escherichia coli', *Curr Top Med Chem*, vol. 18, no. 11, pp. 917–924, 2018.
[20] D. Rubini *et al.*, 'Essential oils from unexplored aromatic plants quench biofilm formation and virulence of Methicillin resistant Staphylococcus aureus', *Microbial Pathogenesis*, vol. 122, pp. 162–173, Sep. 2018.
[21] P. Chemmugil, P. T. V. Lakshmi, and A. Annamalai, 'Exploring Morin as an anti-quorum sensing agent (anti-QSA) against resistant strains of Staphylococcus aureus', *Microb. Pathog.*, vol. 127, pp. 304–315, Feb. 2019.
[22] J.-H. Lee, Y.-G. Kim, S. Yong Ryu, and J. Lee, 'Calcium-chelating alizarin and other anthraquinones inhibit biofilm formation and the hemolytic activity of Staphylococcus aureus', *Sci Rep*, vol. 6, no. 1, p. 19267, May 2016.
[23] C. Nithya, M. G. Devi, and S. Karutha Pandian, 'A novel compound from the marine bacterium Bacillus pumilus S6-15 inhibits biofilm formation in gram-positive and gram-negative species', *Biofouling*, vol. 27, no. 5, pp. 519–528, May 2011.
[24] D. Rubini *et al.*, 'Chitosan extracted from marine biowaste mitigates staphyloxanthin production and biofilms of Methicillin- resistant Staphylococcus aureus', *Food and Chemical Toxicology*, vol. 118, pp. 733–744, Aug. 2018.
[25] K. Pakshir, M. Ravandeh, H. Khodadadi, M. Motamedifar, K. Zomorodian, and S. Alipour, 'Evaluation of Exoenzyme Activities, Biofilm Formation, and Co-hemolytic Effect in Clinical Isolates of Candida parapsilosis Species Complex', *J Glob Infect Dis*, vol. 10, no. 3, pp. 163–165, Sep. 2018.
[26] C. Kong, C.-F. Chee, K. Richter, N. Thomas, N. Abd. Rahman, and S. Nathan, 'Suppression of Staphylococcus aureus biofilm formation and virulence by a benzimidazole derivative, UM-C162', *Sci Rep*, vol. 8, no. 1, p. 2758, Dec. 2018.
[27] S. Kumari, S. Rajit Prasad, D. Mandal, and P. Das, 'Carbon dot-DNA-protoporphyrin hybrid hydrogel for sustained photoinduced antimicrobial activity', *J Colloid Interface Sci*, vol. 553, pp. 228–238, Oct. 2019.
[28] K. Sood, J. Kaur, H. Singh, S. Kumar Arya, and M. Khatri, 'Comparative toxicity evaluation of graphene oxide (GO) and zinc oxide (ZnO) nanoparticles on Drosophila melanogaster', *Toxicol Rep*, vol. 6, pp. 768–781, 2019.
[29] Q. Yi *et al.*, 'Singlet Oxygen Triggered by Superoxide Radicals in a Molybdenum Cocatalytic Fenton Reaction with Enhanced REDOX Activity in the Environment', *Environ. Sci. Technol.*, vol. 53, no. 16, pp. 9725–9733, Aug. 2019.
[30] A. Ganguli, D. Choudhury, S. Datta, S. Bhattacharya, and G. Chakrabarti, 'Inhibition of autophagy by chloroquine potentiates synergistically anti-cancer property of artemisinin by promoting ROS dependent apoptosis', *Biochimie*, vol. 107 Pt B, pp. 338–349, Dec. 2014.
[31] N. R. Cutler, J. J. Sramek, and P. K. Narang, Eds., *Pharmacodynamics and drug development: perspectives in clinical pharmacology*. Chichester: Wiley, 1994.
[32] C. Kaito and K. Sekimizu, 'Colony Spreading in Staphylococcus aureus', *Journal of Bacteriology*, vol. 189, no. 6, pp. 2553–2557, Mar. 2007.
[33] O. Ates, 'Systems Biology of Microbial Exopolysaccharides Production', *Front Bioeng Biotechnol*, vol. 3, p. 200, 2015.

[34] A. Clauditz, A. Resch, K.-P. Wieland, A. Peschel, and F. Götz, 'Staphyloxanthin plays a role in the fitness of Staphylococcus aureus and its ability to cope with oxidative stress', *Infect. Immun.*, vol. 74, no. 8, pp. 4950–4953, Aug. 2006.
[35] B. Fournier and D. J. Philpott, 'Recognition of Staphylococcus aureus by the Innate Immune System', *Clinical Microbiology Reviews*, vol. 18, no. 3, pp. 521–540, Jul. 2005.
[36] H. Strahl and L. W. Hamoen, 'Membrane potential is important for bacterial cell division', *Proceedings of the National Academy of Sciences*, vol. 107, no. 27, pp. 12281–12286, Jul. 2010.
[37] P. Sahariah *et al.*, 'Antimicrobial peptide shows enhanced activity and reduced toxicity upon grafting to chitosan polymers', *Chem. Commun. (Camb.)*, vol. 51, no. 58, pp. 11611–11614, Jul. 2015.
[38] S. Y. C. Tong, J. S. Davis, E. Eichenberger, T. L. Holland, and V. G. Fowler, 'Staphylococcus aureus Infections: Epidemiology, Pathophysiology, Clinical Manifestations, and Management', *Clin. Microbiol. Rev.*, vol. 28, no. 3, pp. 603–661, Jul. 2015.
[39] S. Vora, 'Acute renal failure due to vancomycin toxicity in the setting of unmonitored vancomycin infusion', *Proc (Bayl Univ Med Cent)*, vol. 29, no. 4, pp. 412–413, Oct. 2016.
[40] M. Piechota, B. Kot, A. Frankowska-Maciejewska, A. Grużewska, and A. Woźniak-Kosek, 'Biofilm Formation by Methicillin-Resistant and Methicillin-Sensitive *Staphylococcus aureus* Strains from Hospitalized Patients in Poland', *BioMed Research International*, vol. 2018, pp. 1–7, Dec. 2018.
[41] B. F. Ricciardi, G. Muthukrishnan, E. Masters, M. Ninomiya, C. C. Lee, and E. M. Schwarz, 'Staphylococcus aureus Evasion of Host Immunity in the Setting of Prosthetic Joint Infection: Biofilm and Beyond', *Curr Rev Musculoskelet Med*, vol. 11, no. 3, pp. 389–400, Sep. 2018.
[42] B. Parrino, P. Diana, G. Cirrincione, and S. Cascioferro, 'Bacterial Biofilm Inhibition in the Development of Effective Anti-Virulence Strategy', *Open Med Chem J*, vol. 12, pp. 84–87, 2018.
[43] E. Hodille, W. Rose, B. A. Diep, S. Goutelle, G. Lina, and O. Dumitrescu, 'The Role of Antibiotics in Modulating Virulence in Staphylococcus aureus', *Clin. Microbiol. Rev.*, vol. 30, no. 4, pp. 887–917, Oct. 2017.
[44] K. S. Siddiqi, A. Ur Rahman, null Tajuddin, and A. Husen, 'Properties of Zinc Oxide Nanoparticles and Their Activity Against Microbes', *Nanoscale Res Lett*, vol. 13, no. 1, p. 141, May 2018.
[45] O. M. Bondarenko, M. Sihtmäe, J. Kuzmičiova, L. Ragelienė, A. Kahru, and R. Daugelavičius, 'Plasma membrane is the target of rapid antibacterial action of silver nanoparticles in Escherichia coli and Pseudomonas aeruginosa', *Int J Nanomedicine*, vol. 13, pp. 6779–6790, 2018.
[46] T. Wang, I. El Meouche, and M. J. Dunlop, 'Bacterial persistence induced by salicylate via reactive oxygen species', *Sci Rep*, vol. 7, p. 43839, 10 2017.

## 5. **Figure Legends:**

**Fig.1 –** Characterizations of ZnNPs and ZnNPs-PK. (**A)** Comparative UV-VIS spectra of pancreatin, ZnNPs and ZnNPs-PK by UV-spectrophotometer. **(B)** Comparative analysis of ZnNPs (B1) and ZnNPs-PK(B2) by Dynamic Light Scattering (DLS).

**Fig.2**– Antimicrobial activities of ZnNPs-PK on *MRSA*. **(A)**Graphical representation of comparative antimicrobial activity of ZnNPs and ZnNPs-PK **(B)** Death Kinetics of *MRSA in* presence and absence of ZnNPs-PK.

**Fig.3 –** Anti-biofilms activity by ZnNPs-PK against *MRSA*.**(A)**Tabular representation of effect of ZnNPs-PK on the viability of sessile cells and biofilm biomass of initial and mature biofilms **(B)** Light (B1 and B2) and confocal microscopic (B3 and B4) observation of ZnNPs-PK induced biofilm inhibition

**Fig.4 –** Anti-motility activity by ZnNPs-PK against *MRSA* **(A)** Pictorial representation of inhibition of sliding motility (A1 and A2) and colony motility (A3 and A4) of MRSA by ZnNPs-PK.

**Fig.5 –** Anti-virulence properties of ZnNPs-PK against MRSA **(A)**Pictorial representation of inhibition of slime production of MRSA by ZnNPs-PK. **(A1)** represents untreated cells. **(A2)** represents treated cells. **(B)** Pictorial representation of plasma clamping ability (A3 and A4) of MRSA by ZnNPs-PK. **(B1)** blood plasma with untreated MRSA cells. **(B2)** blood plasma with treated MRSA cells.

**Fig.6** - **(A)** Tabular representation of effect of ZnNPs-PK on exopolysaccharide production, staphyloxanthin production and hemolytic activity of MRSA. **(B)** ROS generation was flow cytometrically evaluated in untreated and ZnNPs-PK treated MRSA cells by using DCFDA.

**Fig.7 –** Mechanism of action of ZnNPs-PK against MRSA **(A)** Membrane potential was flow cytometrically evaluated in untreated and ZnNPs-PK treated MRSA cells by using Rh123 **(B)**

Cell membrane damage was flow cytometrically evaluated in untreated and ZnNPs-PK treated MRSA cells by PI uptake

**Fig.8 –** Ex vivo study and combination study of ZnNPs-PK **(A)** Graphical representation of bioburden of MRSA cells untreated and treated with ZnNPs-PK in porcine skin model. **(B)**Graphical representation of combination activity of ZnNPs-PK and Vancomycin against MRSA

**Figures:**

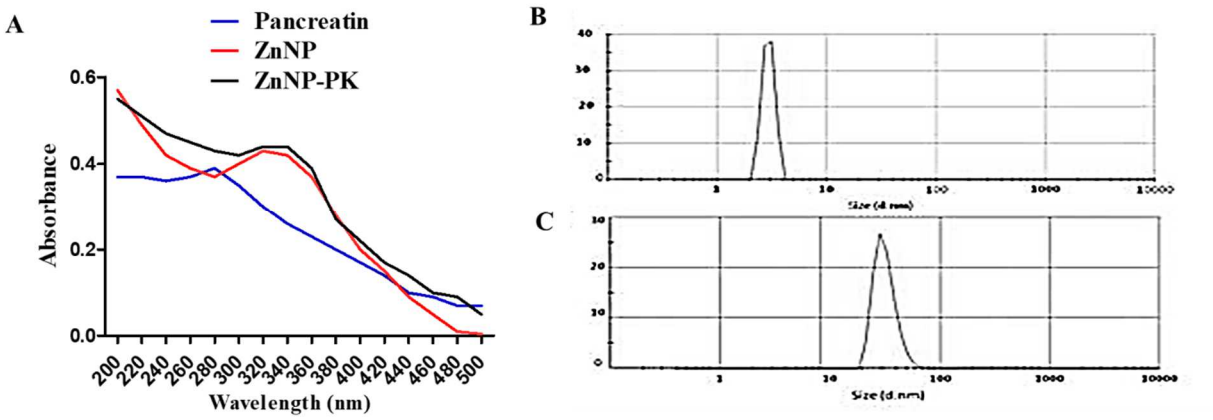


**Fig.1**

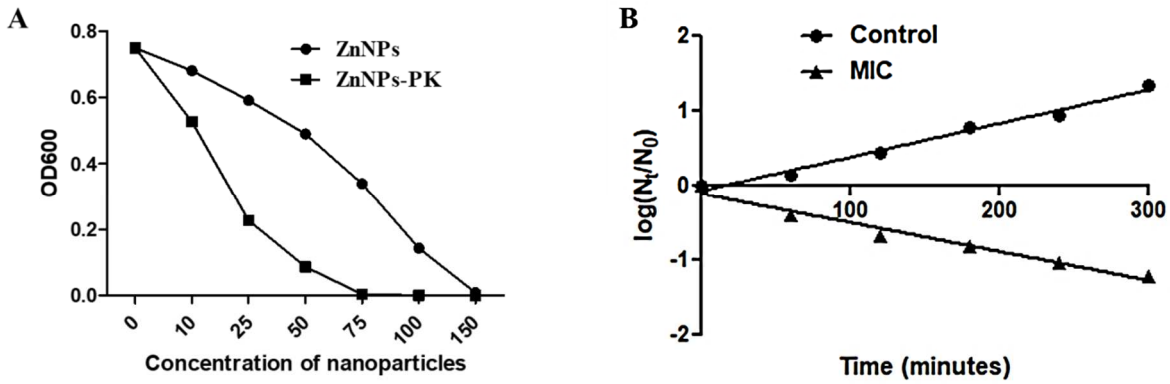


**Fig.2**

A

| | Initial Biofilm | | Mature Biofilm | |
|---|---|---|---|---|
| | CFU/ml | Biomass | CFU/ml | Biomass |
| Control | 8.38 ± 0.67 | 100 | 8.61 ± 0.23 | 100 |
| ½ MIC | 6.6 ± 0.21 | 38 ± 3.2 | 6.8 ± 0.07 | 51 ± 1.1 |
| MIC | 4.2 ± 0.31 | 17 ± 2.7 | 5.1 ± 0.15 | 32 ± 2.4 |

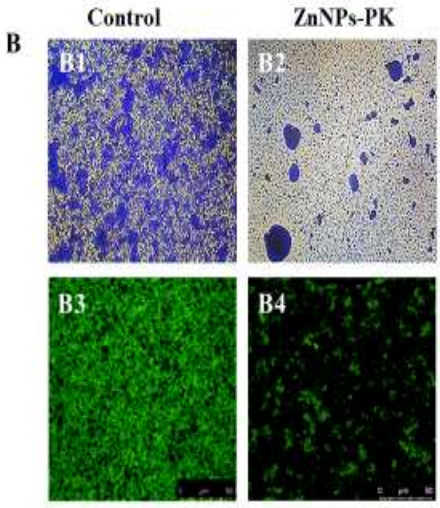


732

733 **Fig.3**

734

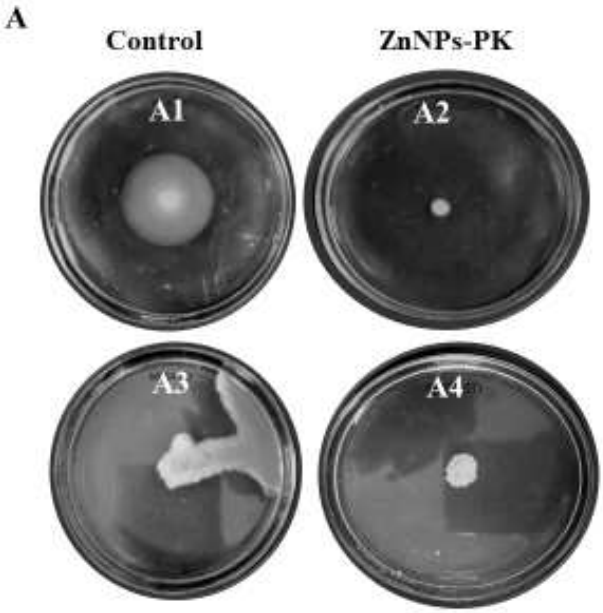


735

736 **Fig. 4**

737

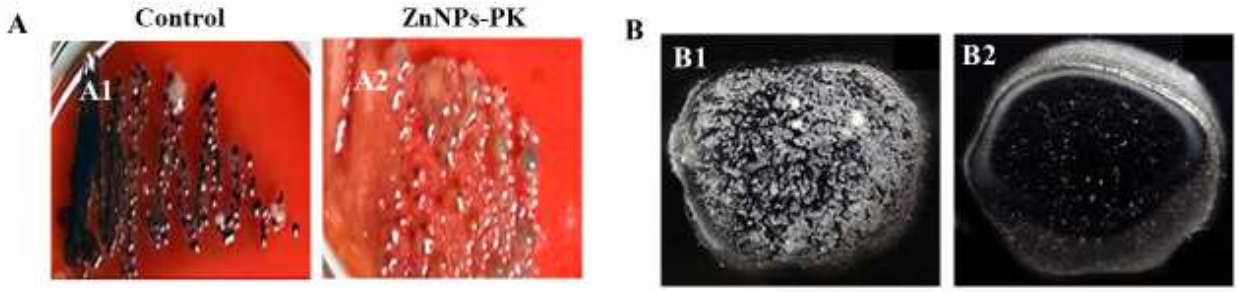


738

739 **Fig. 5**

740

A

| | Control | MIC |
|---|---|---|
| **Exopolysaccharide (OD495nm/ $10^8$ Cells)** | 0.168 ± 0.015 | 0.062 ± 0.009 |
| **Staphyloxanthine (OD462nm/$10^8$ Cells)** | 0.992 ± 0.035 | 0.367 ± 0.053 |
| **Hemolytic Potential (%)** | 100 | 17 ± 2.1 |

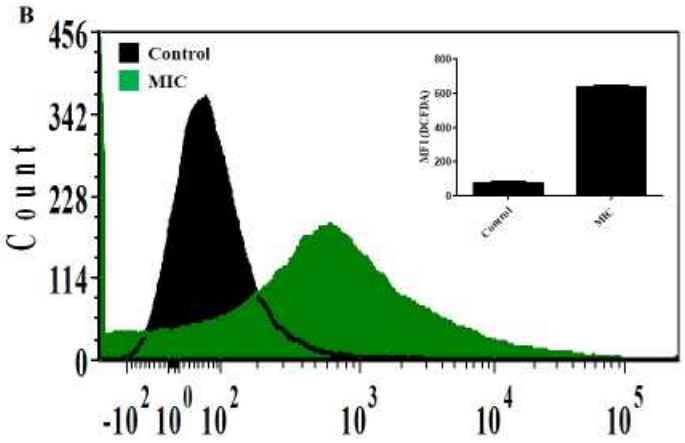


741

742 **Fig.6**

743

744

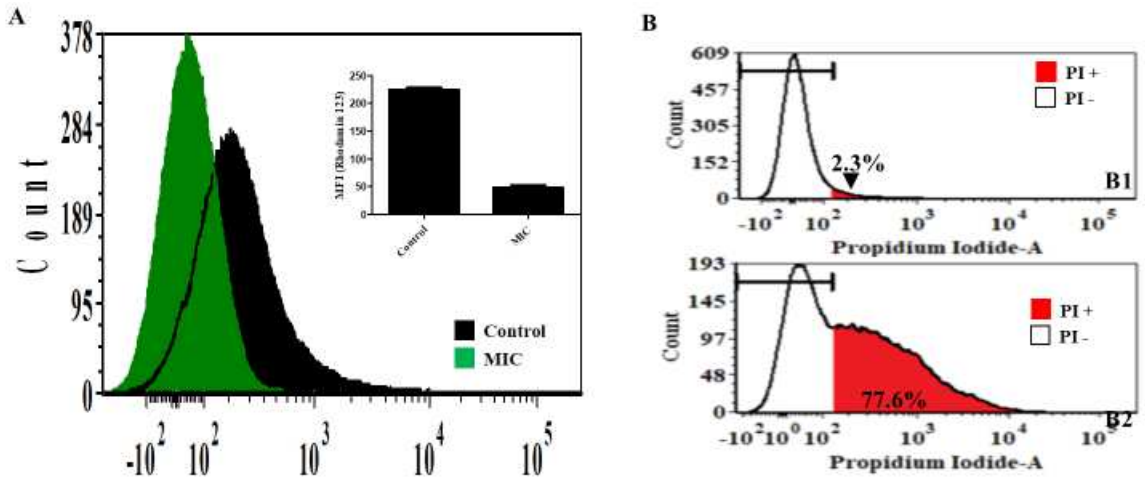


745

746 **Fig.7**

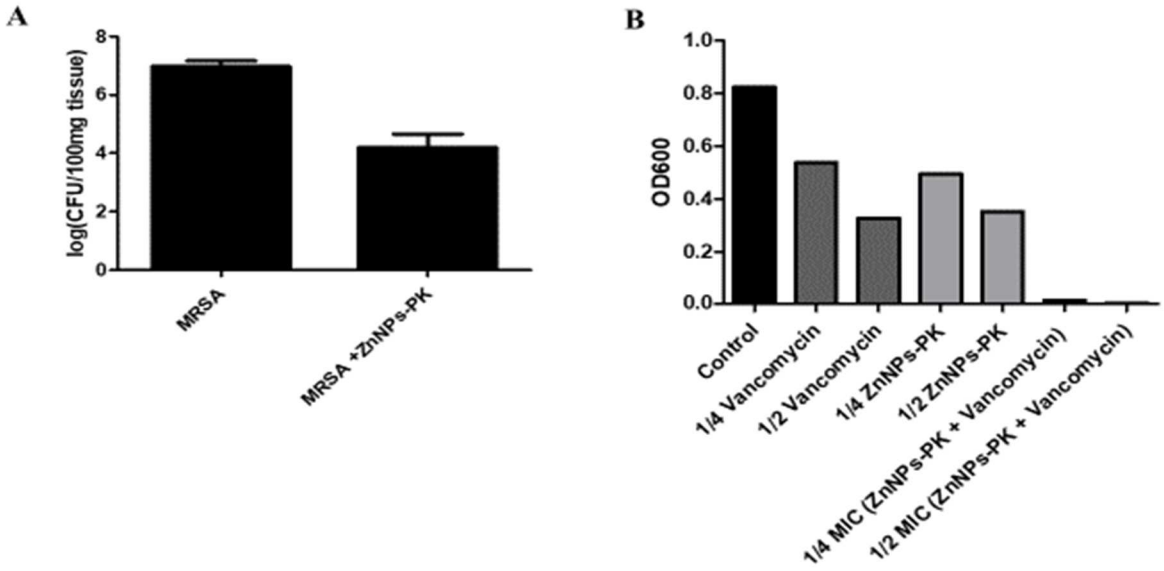


747

748 **Fig. 8**

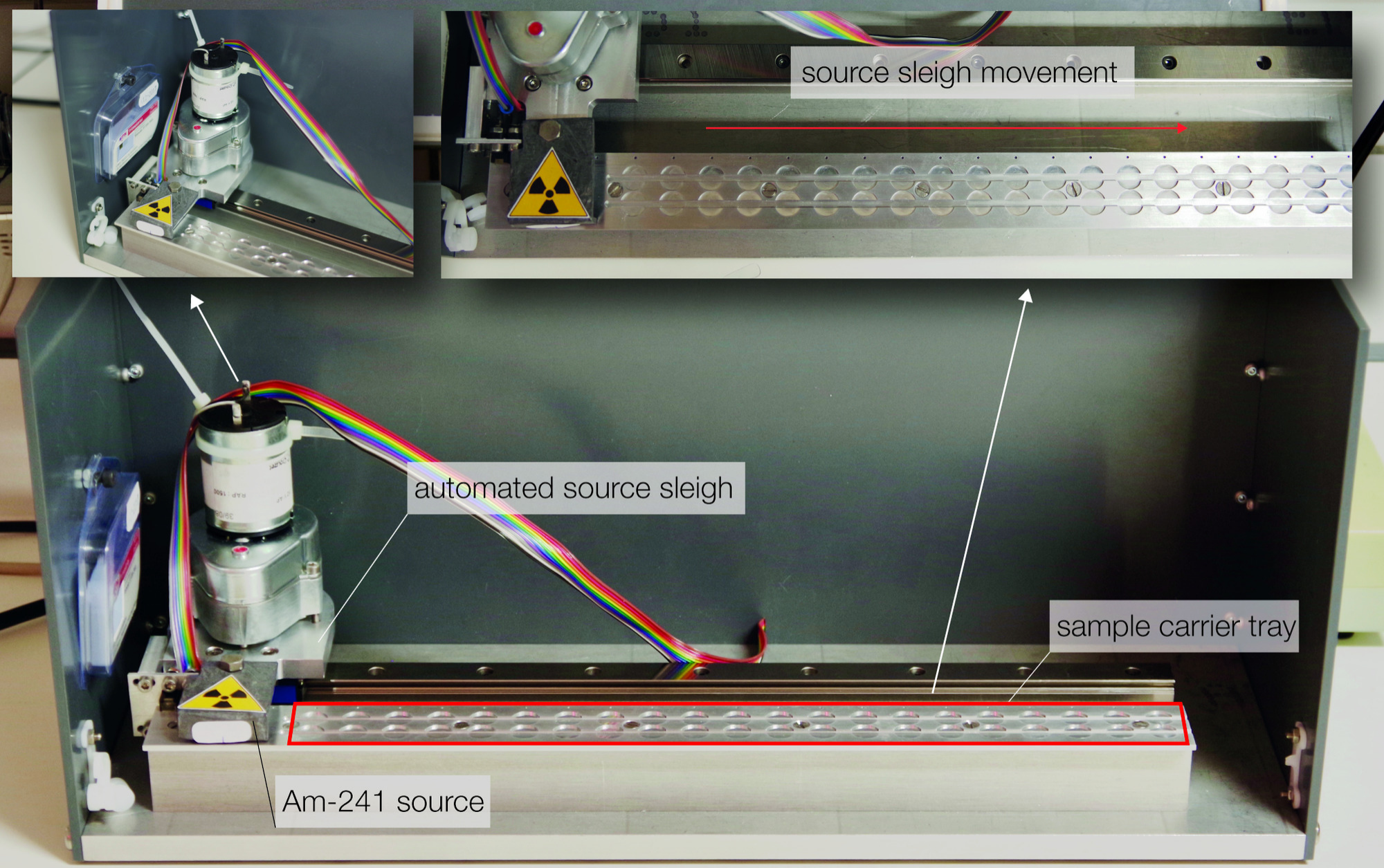


Dimension: 115 x 270 x 124 mm (length x width x height)

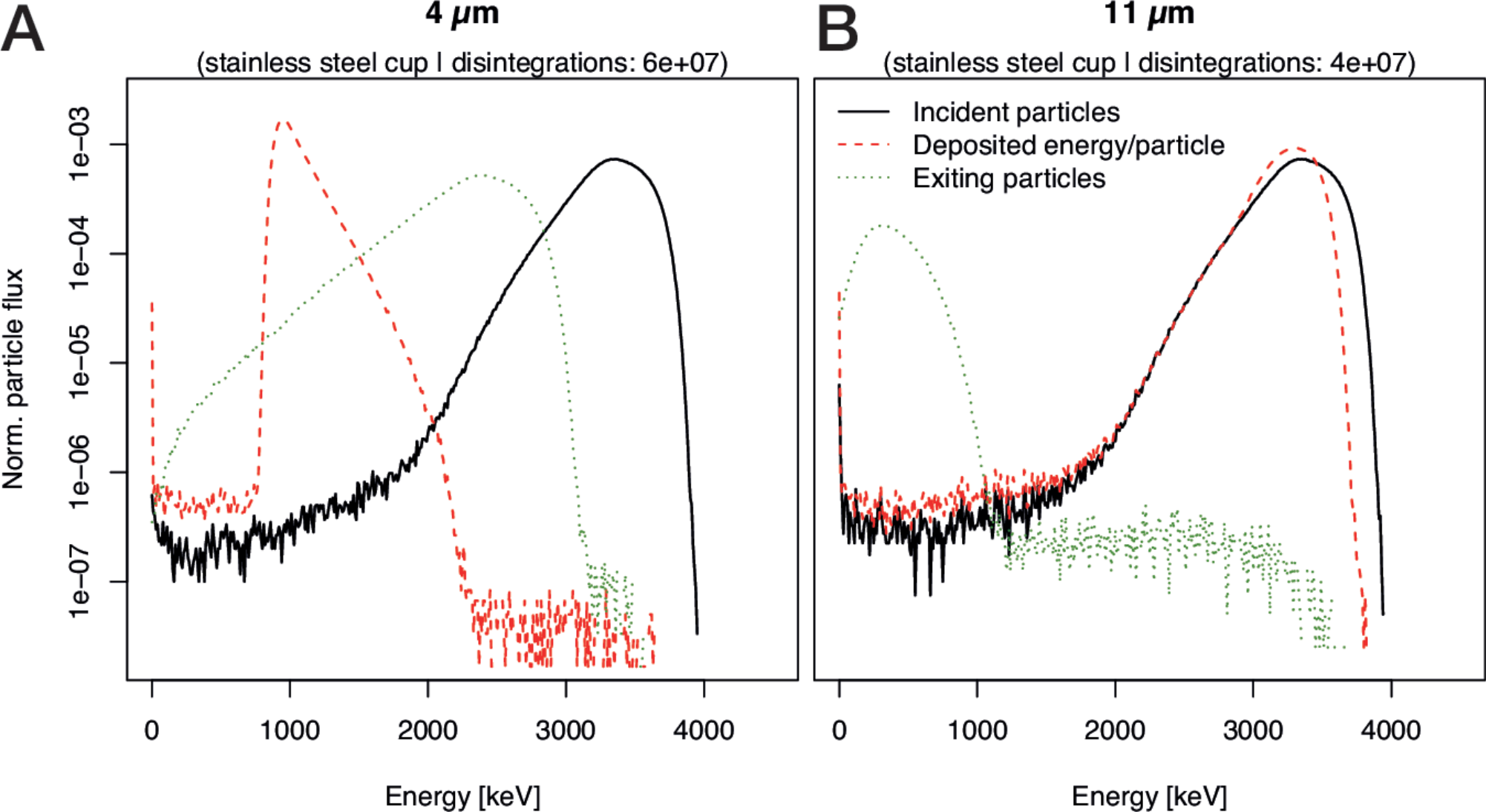
A
4 μm
(stainless steel cup | disintegrations: 6e+07)
B
11 μm
(stainless steel cup | disintegrations: 4e+07)
Incident particles
Deposited energy/particle
Exiting particles
Norm. particle flux
1e−03
1e−04
1e−05
1e−06
1e−07
0
1000
2000
3000
4000
Energy [keV]
Energy [keV]

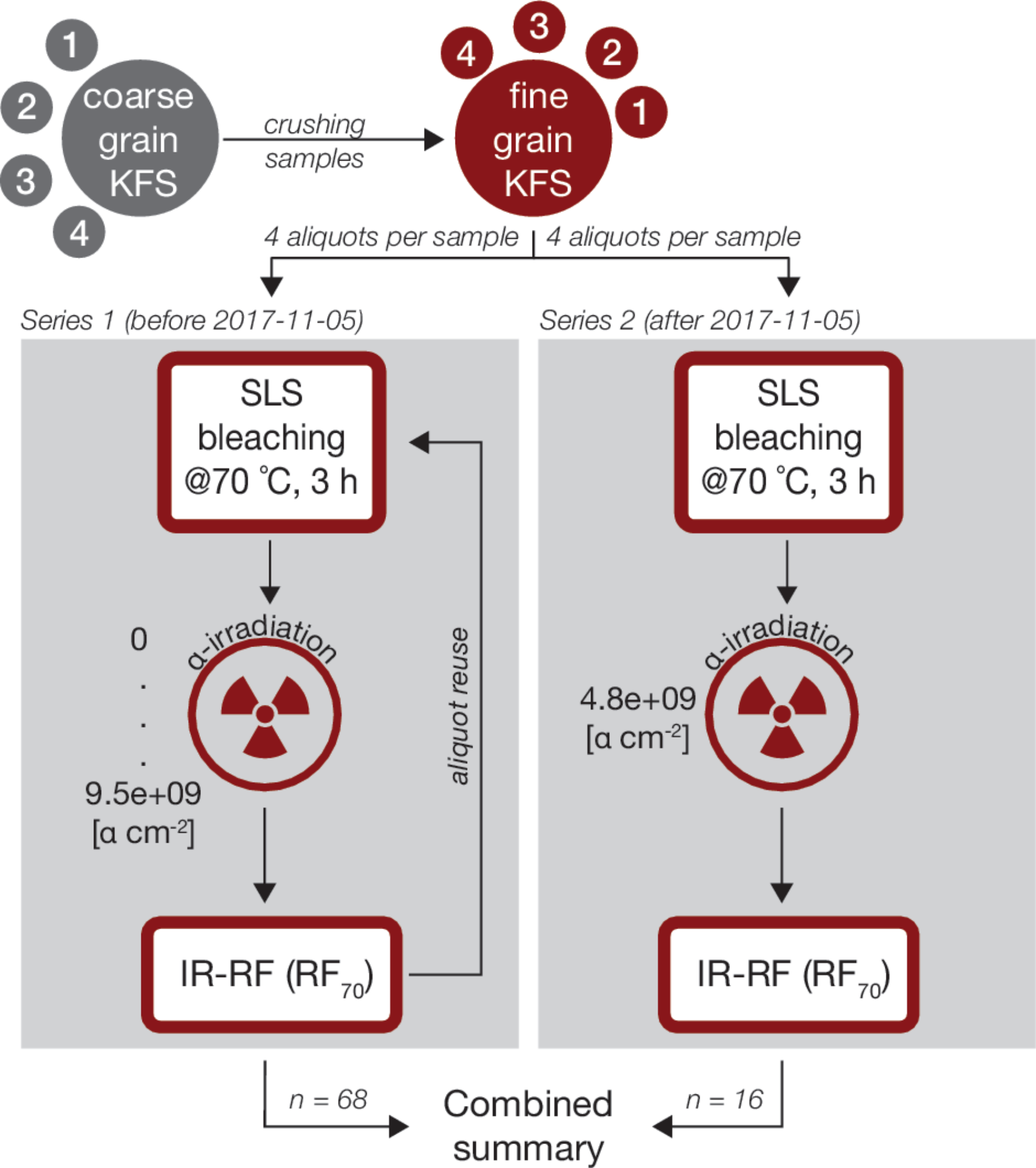
1
2
3
4
coarse grain KFS
crushing samples
3
4
2
1
fine grain KFS
4 aliquots per sample
4 aliquots per sample
Series 1 (before 2017-11-05)
Series 2 (after 2017-11-05)
SLS bleaching @70 °C, 3 h
SLS bleaching @70 °C, 3 h
0
.
.
.
9.5e+09 [α cm-2]
α-irradiation
aliquot reuse
4.8e+09 [α cm-2]
α-irradiation
IR-RF (RF70)
IR-RF (RF70)
n = 68
n = 16
Combined summary

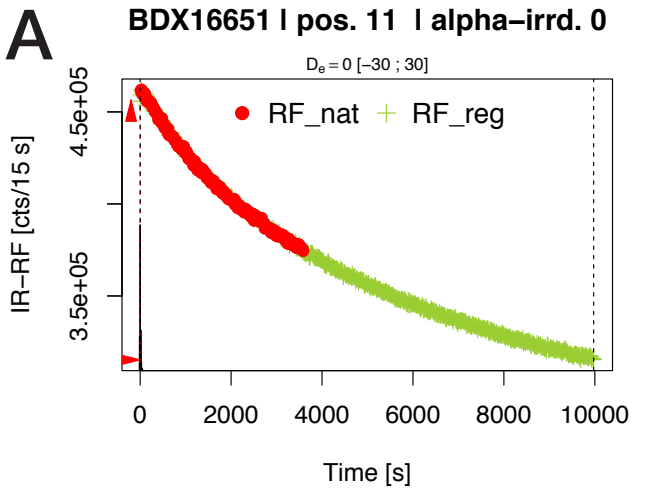
A
BDX16651 | pos. 11 | alpha–irrd. 0
De = 0 [–30 ; 30]
RF_nat
RF_reg
IR–RF [cts/15 s]
4.5e+05
3.5e+05
0
2000
4000
6000
8000
10000
Time [s]

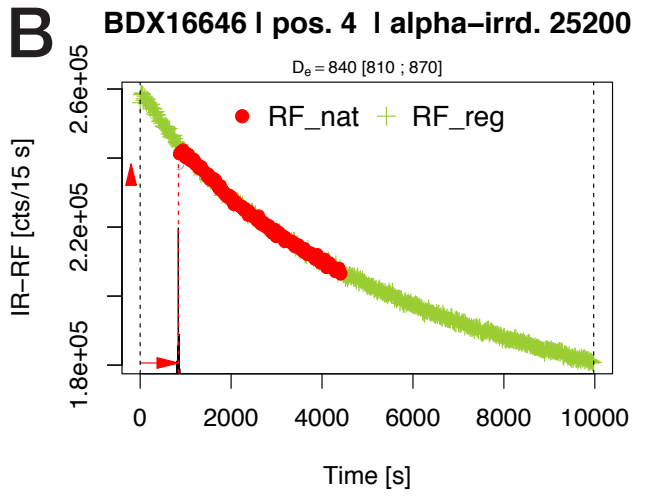
B
BDX16646 | pos. 4 | alpha–irrd. 25200
De = 840 [810 ; 870]
RF_nat
RF_reg
IR–RF [cts/15 s]
2.6e+05
2.2e+05
1.8e+05
0
2000
4000
6000
8000
10000
Time [s]

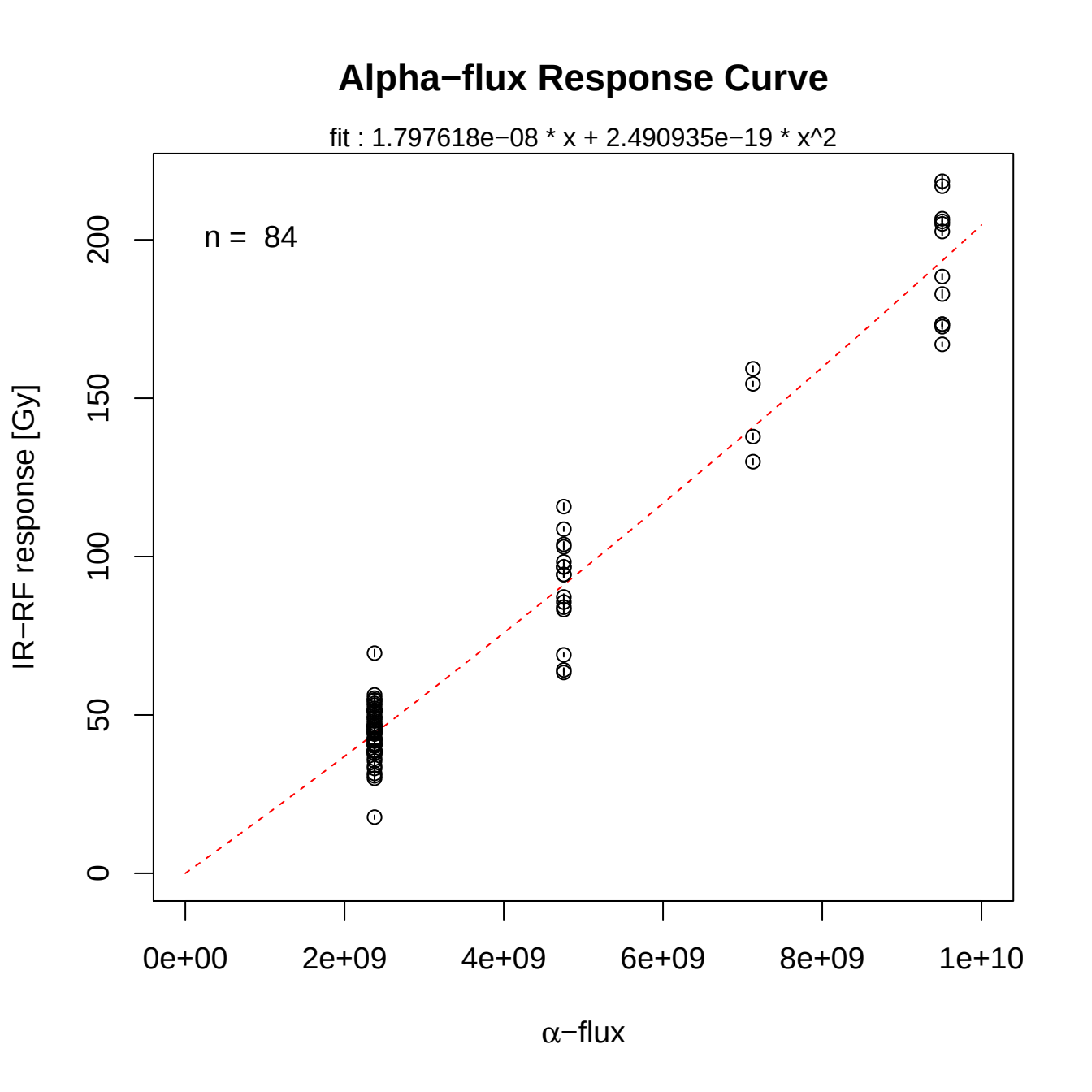
Alpha−flux Response Curve
fit : 1.797618e−08 * x + 2.490935e−19 * x^2
n = 84
IR−RF response [Gy]
0
50
100
150
200
0e+00
2e+09
4e+09
6e+09
8e+09
1e+10
α−flux

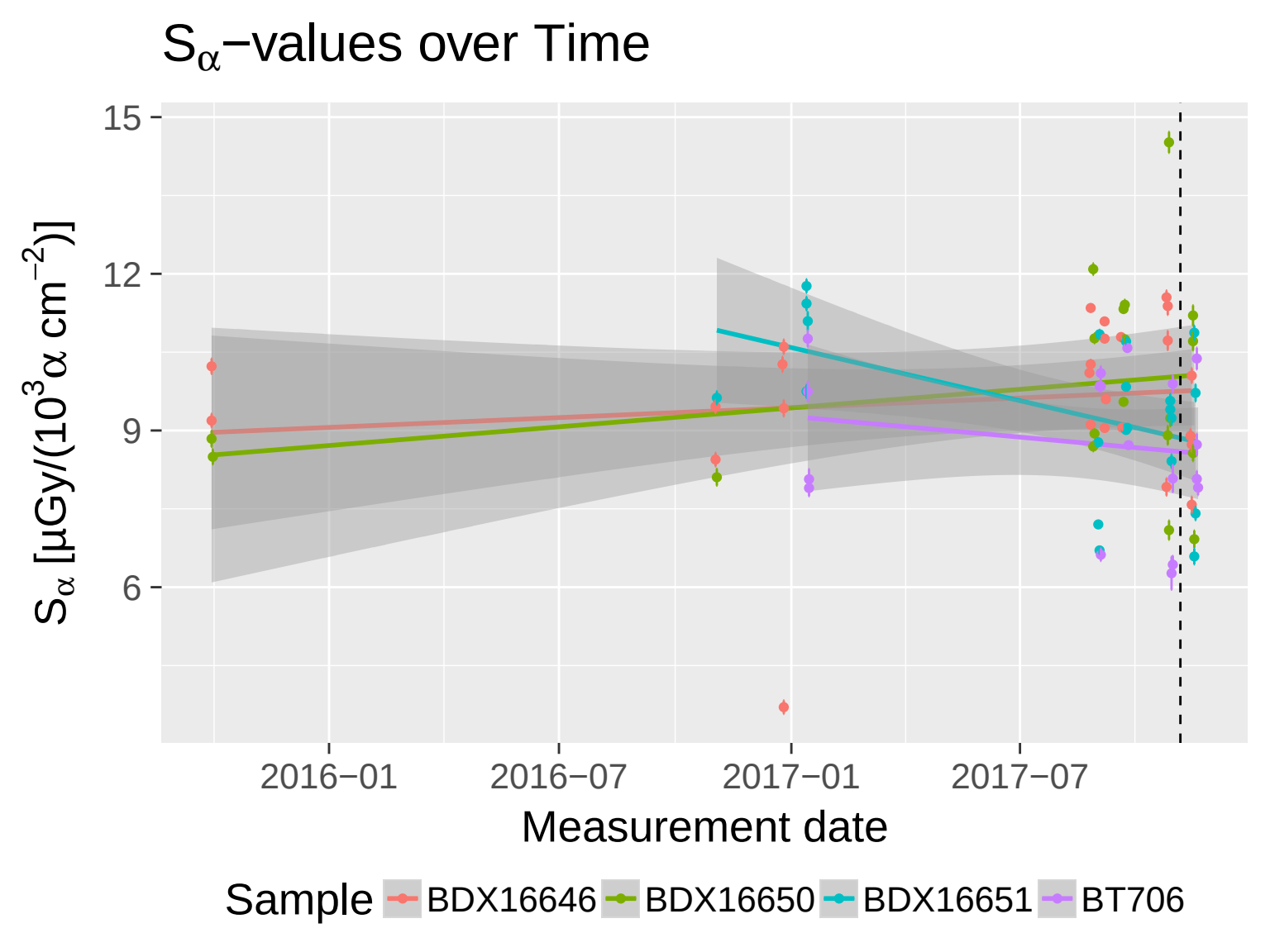
Sα−values over Time
15
12
9
6
Sα [μGy/(10^3α cm^−2)]
2016−01
2016−07
2017−01
2017−07
Measurement date
Sample
BDX16646
BDX16650
BDX16651
BT706

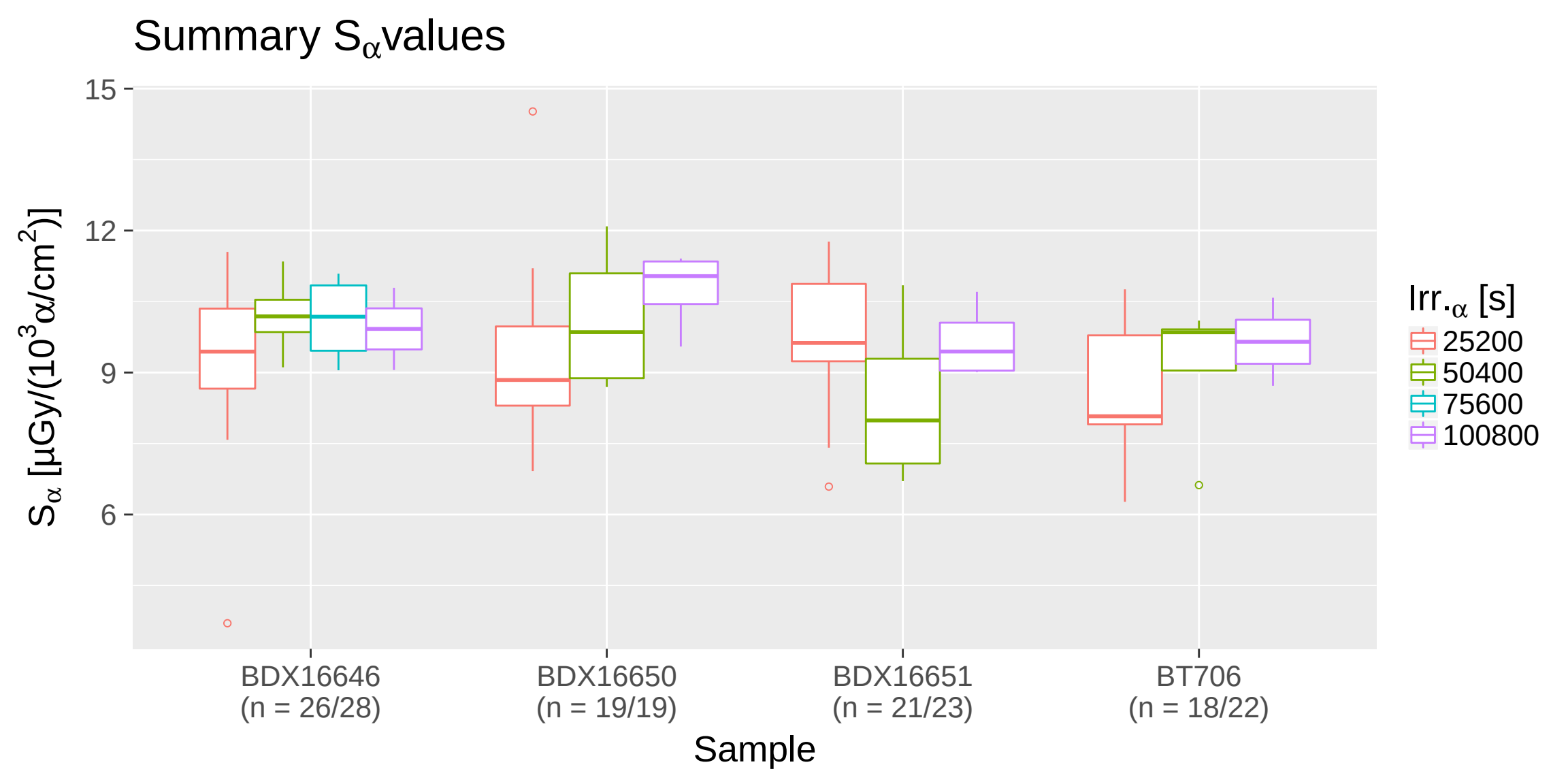
Summary $S_\alpha$values
15
12
9
6
$S_\alpha$ [µGy/($10^3$α/$cm^2$)]
BDX16646
(n = 26/28)
BDX16650
(n = 19/19)
BDX16651
(n = 21/23)
BT706
(n = 18/22)
Sample
Irr.$_\alpha$ [s]
25200
50400
75600
100800

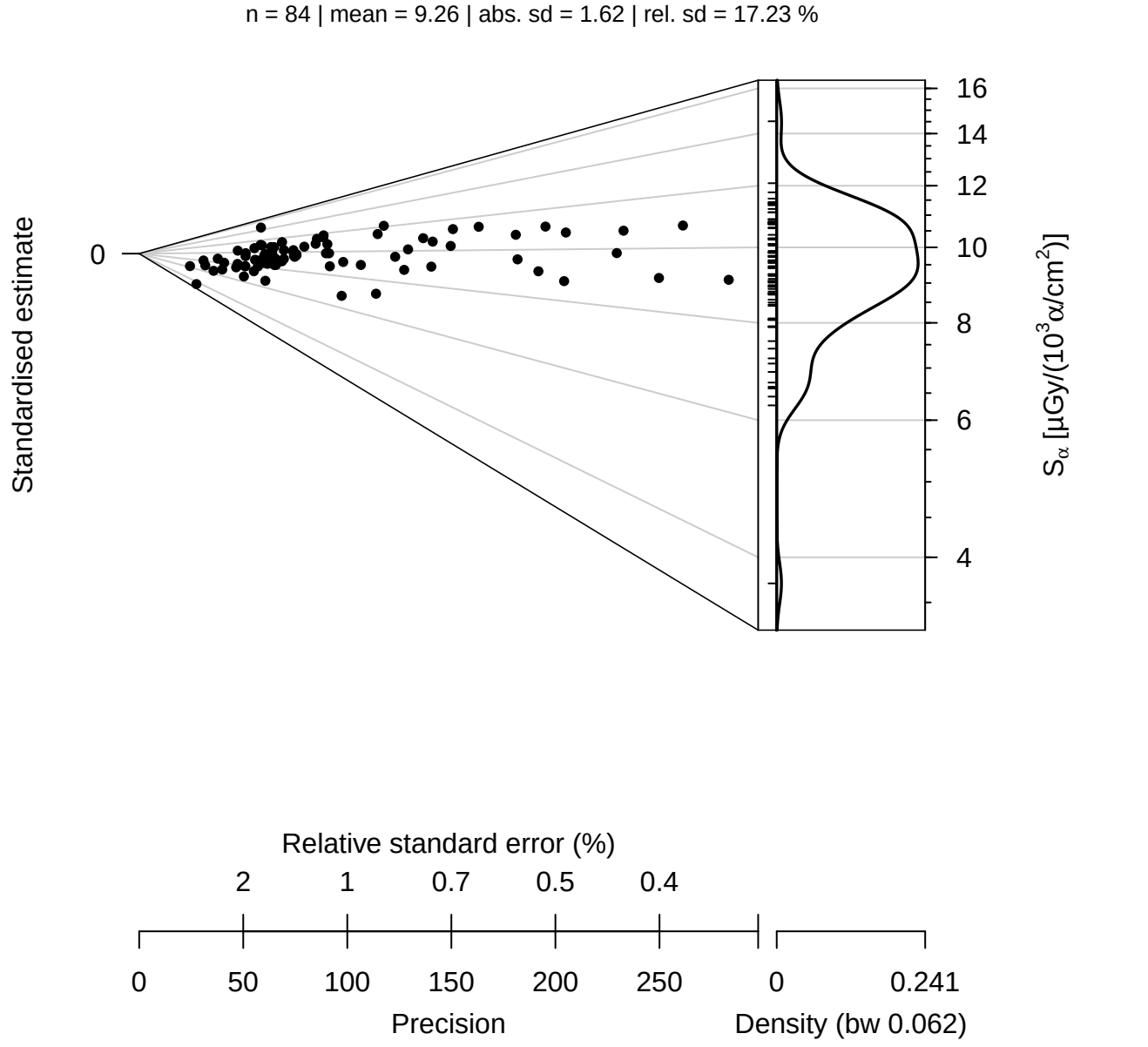
n = 84 | mean = 9.26 | abs. sd = 1.62 | rel. sd = 17.23 %
Standardised estimate
0
16
14
12
10
8
6
4
$S_\alpha$ [µGy/($10^3$α/$cm^2$)]
Relative standard error (%)
2
1
0.7
0.5
0.4
0
50
100
150
200
250
Precision
0
0.241
Density (bw 0.062)

**Table 1**

| SAMPLE | N | $S_\alpha$ [µGy/($10^3\alpha$ $cm^{-2}$)] | SE($S_\alpha$) [µGy/($10^3\alpha$ $cm^{-2}$)] | CV [%] |
|---|---|---|---|---|
| BDX16646 | 26/28 | 10.0 | 1.2 | 12.4 |
| BDX16650 | 19/19 | 10.0 | 1.3 | 13.0 |
| BDX16651 | 21/23 | 9.2 | 1.2 | 12.8 |
| BT706 | 18/22 | 9.0 | 1.2 | 13.2 |

*Note: All values are given as error weighted mean. SE is the standard deviation of the sampling distribution.*